J|A|C|S
COMMUNICATIONS

Published on Web 03/18/2006

Metal-Chelate Dye-Controlled Organization of $Cd_{32}S_{14}(SPh)_{40}^{4-}$ Nanoclusters into Three-Dimensional Molecular and Covalent Open Architecture

Nanfeng Zheng,[†] Haiwei Lu,[†] Xianhui Bu,[‡] and Pingyun Feng*,[†]

Department of Chemistry, University of California, Riverside, California 92521, and Department of Chemistry and Biochemistry, California State University, 1250 Bellflower Boulevard, Long Beach, California 90840

Received January 1, 2006; E-mail: pingyun.feng@ucr.edu

Because of their interesting and unique structures and properties, chalcogenide tetrahedral clusters have attracted increasing attention.[1−4] Geometrically, chalcogenide tetrahedral clusters generally fall into one of three series: supertetrahedral clusters (T*n*), pentasupertetrahedral clusters (P*n*), and capped tetrahedral clusters (C*n*).[4] In addition to the synthesis of clusters with novel compositions and structures, there has been a strong desire to organize these clusters into open-framework architecture that may have use as nanoporous semiconductors.[4−10] Compared to porous oxides, these chalcogenides are characterized by the integration of open architecture with semiconductivity and might find applications beyond those of traditional insulating oxides.[11,12] Such applications include photocatalysis, photovoltaics, and sensing.

To further promote the potential applications of crystalline porous semiconductors, it is highly desirable to develop composite materials that allow uniform molecular-level integration of crystalline semiconducting frameworks with optically active guest species. The synergistic effects in such composite materials would offer unprecedented properties leading to novel applications. Unfortunately, chalcogenide open frameworks developed thus far generally contain extraframework organic cations (e.g., quaternary ammoniums, protonated amines) or hydrated inorganic cations that do not usually contribute to electronic and optical properties.[4−10]

Here we demonstrate the use of optically active metal-chelate dyes (e.g., $[M(1,10\text{-phenanthroline})_3]^{2+}$ (M = Fe^{2+}, Ru^{2+}), $[Fe(2,2'\text{-bipyridine})_3]^{2+}$) as templates to organize chalcogenide clusters into either molecular crystals (denoted MOL-6 and MOL-7, Table 1) or three-dimensional (3D) covalent open frameworks (denoted COV-10 and COV-11, Table 1) from nanosized $[Cd_{32}S_{14}(SC_6H_5)_{38}]^{2-}$ clusters.

This work represents the first time that II−VI clusters containing as many as 32 Cd^{2+} sites are assembled into covalent superlattices. Prior to this work, nearly all C*n* clusters have been prepared as isolated clusters. Two exceptions are $Cd_{17}S_4(SCH_2CH_2OH)_{26}$ and $Cd_{17}S_4(SC_6H_5)_{24}(CH_3OCS_2)_2)$, both of which are based on Cd-17 clusters (denoted C*1*), the first member in the C*n* series.[13−16]

All materials were synthesized under solvothermal conditions at temperatures between 85 and 150 °C. Cd^{2+} and SPh^- sources are usually in the form of $Cd(SPh)_2$.[17] Thiourea is used as the S^{2-} source. Metal-chelate dyes were prepared by mixing metal cations with corresponding ligands. The solvent is CH_3CN or a mixture of CH_3CN and H_2O in various ratios.

COV-10 and COV-11 reported here represent the first two examples of covalent open frameworks consisting of corner-sharing $[Cd_{32}S_{14}(SC_6H_5)_{38}]^{2-}$ (C2) clusters (Figure 1). Both adopt the 2-fold interpenetrating diamond-type lattice with Cd-32 clusters at the tetrahedral node. Even though the double-diamond-type topology is common,[4] the adoption by large II−VI $[Cd_{32}S_{14}(SC_6H_5)_{38}]^{2-}$ clusters as tetrahedral nodes makes COV-10 and COV-11 exceptional. The large size of the $[Cd_{32}S_{14}(SC_6H_5)_{38}]^{2-}$ cluster leads to large extraframework space occupied by cationic metal complexes. In comparison, no extraframework space is present in the $Cd_{17}S_4(SCH_2CH_2OH)_{26}$ framework.[13] The symmetry difference between COV-10 and COV-11 might result from the disorder of the framework phenyl groups and the metal-chelate dyes.

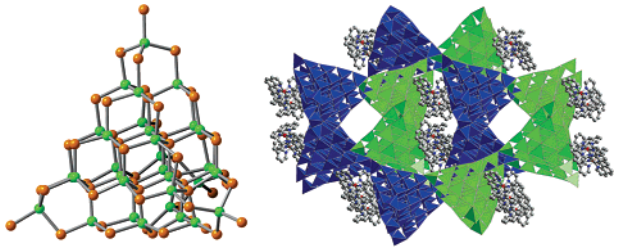

Figure 1. (Left) C2 cluster $[Cd_{32}S_{14}(SPh)_{38}]^{2-}$ in COV-10 and COV-11. Green sphere: Cd^{2+}. Orange sphere: S^{2-}. (Right) 3D framework of COV-10CdS-FePAL. Two interpenetrating lattices are represented in green and blue tetrahedra, respectively. The template, $[Fe(1,10\text{-phenanthroline})_3]^{2+}$, is shown in ball-and-stick.

The unprecedented covalent superlattices built from Cd-32 clusters result from the unique templating strategy employed for II−VI chalcogenides for the first time. Because of the low charge density of C*n* clusters, the frameworks of COV-10 and COV-11 have considerably lower charge density than those from T*n* (e.g., T5 $In_{22}Zn_{13}S_{54}^{16-}$) or P*n* (e.g., P2 $In_{22}Li_4S_{44}^{18-}$) clusters.[4−10] The use of metal-chelate dyes as templates is therefore essential for the synthesis of the covalent frameworks based on large Cd-32 clusters. Compared to commonly used protonated amines or inorganic cations, the metal-chelate dyes used here have larger size and lower charge density. This feature makes them ideal to template the formation of superlattices that are also made of low-charge density clusters. In addition, the hydrophobic surface of the metal-chelate dyes also matches well with the hydrophobic surface of the nanoclusters.

The structural and compositional diversity of metal-chelate dyes offers many possibilities in the controlled assembly of different low-charged nanoclusters into open topologies that are not accessible with conventional organic or inorganic templates. The work reported here represents an unprecedented application of the host−guest charge density matching (i.e., global charge matching) in the construction of superlattices from II−VI nanoclusters.

In addition to templating the formation of 3D covalent frameworks, metal-chelate dyes can also induce the crystallization of different tetrahedral clusters and stabilize their molecular lattice. These molecular crystals can be synthesized at a temperature lower than that for covalent framework structures. For example, MOL-6CdS-FePAL was successfully synthesized at 110 °C from the same reaction mixture for COV-10CdS-FePAL that was obtained at 130 °C.[17] In this work, Cd-32 clusters are present in both MOL-6 (Figure

[†] University of California, Riverside.
[‡] California State University.

10.1021/ja060006+ CCC: $33.50

Table 1. Summary of Crystallographic Data in This Study[a]

name[b]	cluster	cluster composition	space group	*a* (Å)	*b* (Å)	*c* (Å)	*β* (deg)	*R*1
COV-10CdS-FePAL	C2 CdS	$Cd_{32}S_{14}(SPh)_{38}^{2-}$	*C*2/*c*	48.250(2)	48.650(2)	35.652(2)	131.386(2)	6.28
COV-10CdS-RuPAL	C2 CdS	$Cd_{32}S_{14}(SPh)_{38}^{2-}$	*C*2/*c*	48.448(6)	48.899(7)	35.851(5)	131.502(3)	6.13
COV-11CdS-FeBPy	C2 CdS	$Cd_{32}S_{14}(SPh)_{38}^{2-}$	*Fddd*	46.374(2)	51.581(2)	53.407(2)	90	7.61
MOL-6CdS-FePAL	C2,1 CdS	$Cd_{32}S_{14}(SPh)_{40}^{4-}$	$P2_1/c$	20.9325(4)	46.3439(9)	34.2172(7)	92.061(1)	9.67
MOL-7CdS-FeTMPAL	C2,1 CdS	$Cd_{32}S_{14}(SPh)_{40}^{4-}$	$P\bar{1}$	21.588(4)	22.323(4)	43.844(9)	78.61(3)	6.83

[a] Diffraction data were collected on a Bruker APEX diffractometer with Mo Kα X-ray source at 90−150 K. The final full-matrix refinements were against F^2. $R(F) = \sum||F_o| - |F_c||/\sum |F_o|$ with $F_o > 4.0\sigma(F)$. For MOL-7CdS FePAL, $\alpha = 76.220(30)°$; $\gamma = 84.380(30)°$. [b] FePAL = $[Fe(1,10\text{-phenanthroline})_3]^{2+}$; RuPAL = $[Ru(1,10\text{-phenanthroline})_3]^{2+}$; FeTMPAL = $[Fe(3,4,7,8\text{-tetramethyl-}1,10\text{-phenanthroline})_3]^{2+}$; FeBPy = $[Fe(2,2'\text{-bipyridine})_3]^{2+}$. Due to disorder of surface capping phenyl groups, it is not possible to obtain accurate bond lengths involving carbon atoms.

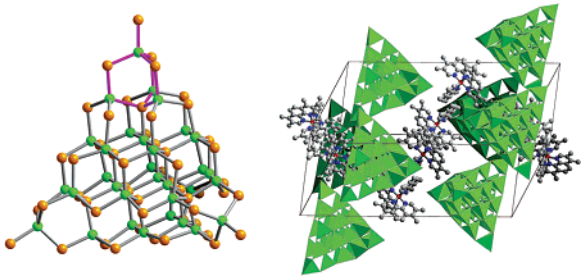

Figure 2. (Left) Individual C*2,1* cluster $[Cd_{32}S_{14}(SPh)_{40}]^{4-}$ in MOL-6 and MOL-7. Green sphere: Cd^{2+}. Orange sphere: S^{2-}. The rotated barrelanoid cage is highlighted by purple-colored bonds. (Right) Structure of MOL-6. C*2,1* clusters are shown in green tetrahedra. The template, $[Fe(1,10\text{-phenanthroline})_3]^{2+}$, is shown in ball-and-stick.

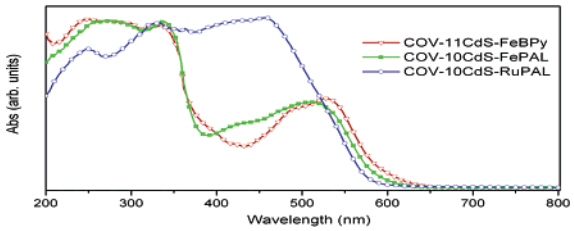

Figure 3. UV−vis absorption spectra for selected compounds.

2) and MOL-7. It is worth noting that, compared to the Cd-32 cluster in COV-10 and COV-11, each Cd-32 cluster in MOL-6 and MOL-7 has one of four barrelanoid cages rotated by 60° and is therefore denoted as C*2,1* cluster.[4] While $[Fe(1,10\text{-phenanthroline})_3]^{2+}$ controls the packing mode in MOL-6, larger $[Fe(3,4,7,8\text{-tetramethyl-}1,10\text{-phenanthroline})_3]^{2+}$ controls the formation of MOL-7.

More importantly, the co-assembly of optically active species, metal-chelate dyes in this work, with molecular or covalent semiconductor superlattices of chalcogenide nanoclusters opens new opportunities for the control of electronic or optical properties of resulting hybrid materials. As illustrated in Figure 3, the composite materials synthesized here from metal-chelate dyes and CdS nanoclusters exhibit significant visible light absorption that is quite sensitive to the nature of the metal-chelate dyes. The absorption properties could be tuned by changing either the type of metal centers or organic ligands. This interesting property might make them useful candidates as visible light photocatalysts or photocurrent generators.

In conclusion, metal-chelate dyes have been demonstrated as effective structure-directing agents to control the organization of relatively low-charged chalcogenide nanoclusters into nanocluster open frameworks that are not accessible by other templating methods. The resulting chalcogenide open frameworks exhibit interesting optical properties that reflect the combined effects of both metal-chelate dyes and semiconducting open frameworks.

Acknowledgment. We thank for the support of this work by the NSF (P.F.), Beckman Foundation (P.F.), and the donors of the Petroleum Research Fund (administered by the ACS) (X.B.). P.F. is a Camille Dreyfus Teacher-Scholar.

Supporting Information Available: Crystallographic data including positional parameters, thermal parameters, and bond distances and angles (CIF, PDF). This material is available free of charge via the Internet at http://pubs.acs.org.

References

(1) Dance, I. G.; Fisher, K. *Prog. Inorg. Chem.* **1994**, *41*, 637−803.
(2) Krebs, B.; Henkel, G. *Angew. Chem., Int. Ed.* **1991**, *30*, 769−788.
(3) Corrigan, J. F.; Degroot, M. W. In *The Chemistry of Nanomaterials: Synthesis, Properties and Applications*; Rao, C. N. R., Müller, A., Cheetham, A. K., Eds.; Wiley: Weinheim, 2004; Vol.2, pp 418−451.
(4) (a) Feng, P.; Bu, X.; Zheng, N. *Acc. Chem. Res.* **2005**, *38*, 293−303. (b) Zheng, N.; Bu, X.; Lu, H.; Zhang, Q.; Feng, P. *J. Am. Chem. Soc.* **2005**, *127*, 11963−11965.
(5) (a) Cahill, C. L.; Parise, J. B. *J. Chem. Soc., Dalton Trans.* **2000**, 1475−1482. (b) Cahill, C. L.; Ko, Y.; Parise, J. B. *Chem. Mater.* **1998**, *10*, 19−21.
(6) (a) Li, H.; Laine, A.; O'Keeffe, M.; Yaghi, O. M. *Science* **1999**, *283*, 1145−1147. (b) Li, H.; Kim, J.; Groy, T. L.; O'Keeffe, M.; Yaghi, O. M. *J. Am. Chem. Soc.* **2001**, *123*, 4867−4868.
(7) Zheng, N.; Bu, X.; Feng, P. *Nature* **2003**, *426*, 428−432.
(8) Zheng, N.; Bu, X.; Wang, B.; Feng, P. *Science* **2002**, *298*, 2366−2369.
(9) Zheng, N.; Bu, X.; Feng, P. *Angew. Chem., Int. Ed.* **2004**, *43*, 4753−4755.
(10) Manos, M. J.; Iyer, R. G.; Quarez, E.; Liao, J. H.; Kanatzidis, M. G. *Angew. Chem., Int. Ed.* **2005**, *44*, 3552−3555.
(11) Dhingra, S.; Kanatzidis, M. G. *Science* **1992**, *258*, 1769−1772.
(12) Scott, R. W. J.; MacLachlan, M. J.; Ozin, G. A. *Curr. Opin. Solid State Mater. Sci.* **1999**, *4*, 113−121.
(13) (a) Vossmeyer, T.; Reck, G.; Katsikas, L.; Haupt, E. T. K.; Schulz, B.; Weller, H. *Science* **1995**, *267*, 1476−1479. (b) Jin, X.; Tang, K.; Jia, S.; Tang, Y. S *Polyhedron* **1996**, *15*, 2617−2218.
(14) Herron, N.; Calabrese, J. C.; Farneth, W. E.; Wang, Y. *Science* **1993**, *259*, 1426−1428.
(15) Vossmeyer, T.; Reck, G.; Schulz, B.; Katsikas, L.; Weller, H. *J. Am. Chem. Soc.* **1995**, *117*, 12881−12882.
(16) Behrens, S.; Bettenhausen, M.; Deveson, A. C.; Eichhoefer, A.; Fenske, D.; Lohde, A.; Woggon, U. *Angew. Chem., Int. Ed.* **1996**, *35*, 2215−2218.
(17) A typical synthesis condition is given below using COV-10CdS-FePAL as an example. A solution containing 67 mg of $FeCl_2$, 283 mg of 1,10-phenanthroline, and 25.122 g of CH_3CN was prepared. A quantity of 2.557 g of this solution, 85 mg of $Cd(SPh)_2$, 41 mg of thiourea, and 0.508 g of water were then mixed in a 23-mL Teflon-lined stainless steel autoclave and stirred for ∼20 min. The vessel was then sealed and heated at 130 °C for 5 days. After cooling to room temperature, crystals of COV-10CdS-FePAL were obtained as red crystals.

JA060006+